32nd Electric Vehicle Symposium (EVS32)
Lyon, France, May 19 - 22, 2019

Analysis of Optimal Battery State-of-Charge Trajectory for Blended Regime of Plug-in Hybrid Electric Vehicle

Branimir Škugor[1], Jure Soldo[2] and Joško Deur[3]

[1,2,3]*University of Zagreb, Faculty of Mechanical Engineering and Naval Architecture, Ivana Lučića 5, Zagreb, Croatia*

Email: [1]branimir.skugor@fsb.hr, [2]jure.soldo@fsb.hr, [3]josko.deur@fsb.hr

Summary

The paper deals with an analysis of optimal battery state-of-charge (SoC) trajectory profile for plug-in hybrid electric vehicles (PHEV). The case of blended operating regime is considered, where hybrid driving mode is enabled during the whole trip. The analysis relates to a SoC trajectory length minimization pattern observed in optimal SoC trajectories obtained by using dynamic programming-based optimisation of PHEV powertrain control variables. The emphasis is on analytical interpretation of the optimal SoC trajectory pattern from the perspectives of simplified battery-only system and the whole PHEV powertrain. Also, the impact of engine specific fuel consumption characteristic on the optimal SoC trajectory solution is analysed.

Keywords: Plug-in hybrid electric vehicle, battery state of charge, powertrain, efficiency, optimisation, power management.

1 Introduction

Plug-in hybrid electric vehicles (PHEV) are proven to be viable transition technology towards fully electric vehicles (EV), as they overcome main deficiencies of EVs such as high prices and short range, while allowing recharging from power grid. PHEVs typically operate in charge depleting (CD) and charge sustaining (CS) regimes, where pure electric (CD) driving is active until the battery is discharged to a predefined lower-limit level, when hybrid driving (CS) is activated in order to sustain the battery state-of-charge (SoC). In the case of knowing a trip length in advance, it is possible to discharge the battery more gradually under blended regime (BLND) and thus further reduce fuel consumption [1, 2, 3] (typically from 2% to 5% when compared to the CD/CS regime [1]). The optimal SoC trajectory (expressed with respect to travelled distance) tends to have a nearly-linear minimum-length shape for the zero road grade case [1, 2, 3], while it can significantly deviate from the linear trend in the presence of variable road grade [1, 3], low emission zones [4], and different driving patterns on different route segments [2].

This paper deals with an analysis of optimal SoC trajectory profiles obtained by using dynamic programming (DP) optimisation of PHEV control variables in the blended regime. A convex analysis of the relevant powertrain functions is conducted to explain the observed optimal SoC trajectory patterns, in order to further gain insights into the optimal powertrain operation for different operating conditions.

The main contributions of the paper include: (i) proposing a method of generating optimal SoC trajectories of different length and conducting correlation analyses of obtained results, (ii) clarifying the cause and conditions under which the optimal SoC trajectory has a minimum-length linear pattern, and (iii) analytical proof of optimal SoC trajectory pattern for the simplified scenarios of battery-only discharging system.

2 Modelling of PHEV Powertrain

Fig. 1a illustrates the parallel PHEV configuration of a city bus powertrain considered herein for the purpose of analysis. The powertrain consists of internal combustion engine (ICE), electric machine (M/G), lithium-ion battery and automated manual transmission with 12 gears [5]. When being switched off, the engine can be disconnected from the powertrain by using a clutch, thus enabling electric-only driving. The PHEV powertrain is modelled in the backward-looking manner, where the engine i.e. M/G machine rotational speed $\omega_e = \omega_{MG}$ is calculated from the vehicle velocity v_v:

$$\omega_e = \omega_{MG} = i_o h \omega_w = i_o h \frac{v_v}{r_w}, \tag{1}$$

while the total engine and M/G machine torque is obtained from the demanded torque at wheels τ_w while accounting from the drivetrain losses:

$$\tau_e + \tau_{MG} = \frac{\tau_{cd}}{i_o h} = \frac{\left(\frac{\tau_w}{\eta_{tr}(\tau_w)} + \frac{P_0(\omega_w)}{\omega_w}\right)}{i_o h}. \tag{2}$$

In Eqs. (1) and (2) h and i_o denote the transmission gear ratio and the final drive ratio, respectively, ω_w is the wheel speed, r_w is the effective tire radius, η_{tr} is the transmission efficiency, while P_0 denotes the idle-mode power losses (see Figs. 1b and 1c). The demanded power can then be defined as

$$P_d = \omega_w \tau_{cd} = \frac{\omega_w \tau_w}{\eta_{tr}(\tau_w)} + P_0(\omega_w) \tag{3}$$

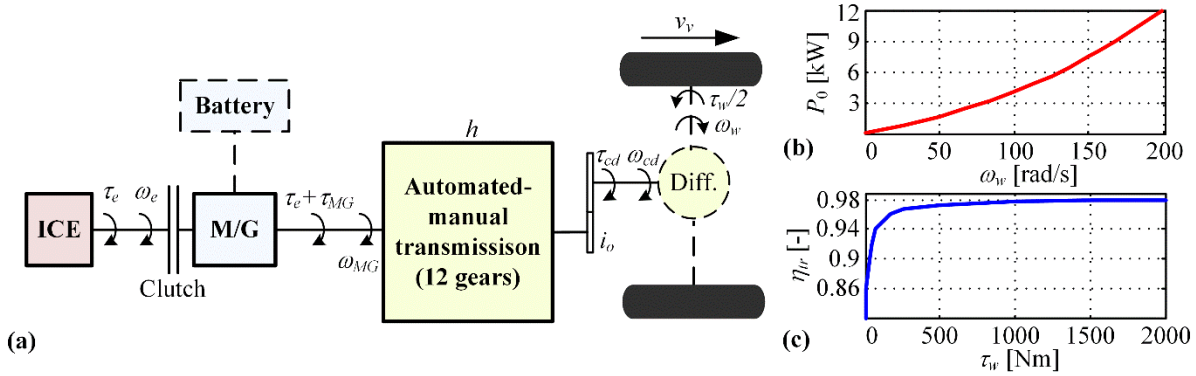

Figure 1: Parallel PHEV powertrain configuration (a), transmission idle-mode power loss map (b), and mechanical efficiency map (c).

The engine specific fuel consumption and M/G machine efficiency are modelled by means of 2D maps, while the corresponding maximum torque characteristics are modelled by 1D maps (Fig. 2). The specific fuel consumption map (A_{ek}), expressed in g/kWh unit, can readily be transformed to the fuel consumption rate map ($\dot{m}_f$; expressed in g/s unit) by using the following expression:

$$\dot{m}_f = A_{ek}(\tau_e, \omega_e) \frac{\tau_e \omega_e}{3.6 \cdot 10^6}. \tag{4}$$

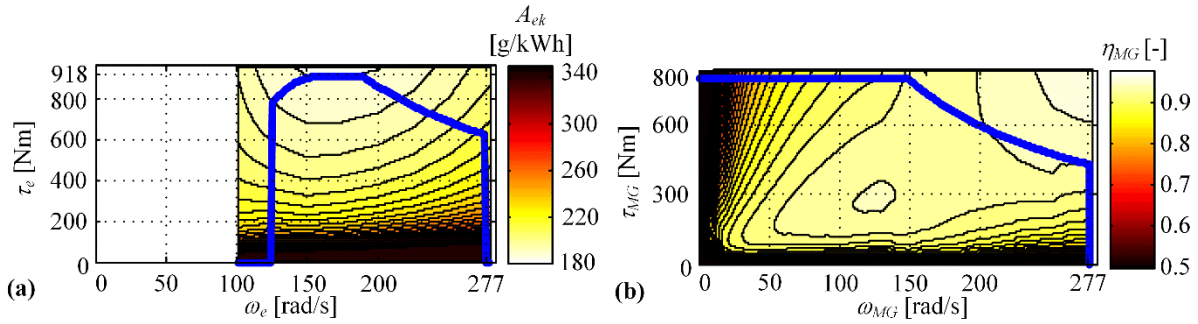

Figure 2: Engine specific fuel consumption map (a), and M/G machine efficiency map (b), given along with maximum torque lines (denoted in blue).

The battery is modelled as a charge storage by an equivalent electrical circuit (Fig. 3a), where the open circuit voltage U_{oc} and internal resistance R are set to be dependent on the battery state-of-charge (SoC) (Fig. 3b). Finally, the battery model is represented by the following state equation [6]

$$\dot{SoC} = \frac{\sqrt{U_{oc}^2(SoC) - 4R(SoC)P_{batt}} - U_{oc}(SoC)}{2Q_{max}R(SoC)}, \tag{5}$$

where Q_{max} is the battery charge capacity, while P_{batt} is the battery power which is determined by M/G machine power P_{MG} as

$$P_{batt} = \eta_{MG}^{k} \underbrace{\tau_{MG}\omega_{MG}}_{P_{MG}}, \tag{6}$$

where η_{MG} denotes M/G machine efficiency (see Fig. 2b), and k is equal to 1 for the case of battery charging (P_{batt}<0) and −1 for the case of battery discharging (P_{batt}>0).

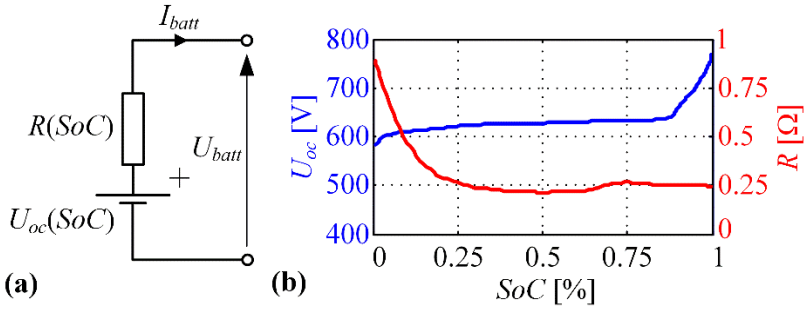

Figure 3: Battery equivalent circuit (a), and open-circuit voltage and internal battery resistance dependences on battery SoC for considered lithium iron phosphate battery (b).

3 Optimisation of PHEV Control Variables

This section deals with DP optimisation of PHEV control variables for the blended regime, which is aimed at finding optimal SoC trajectories for different driving cycles and conditions. More details on the optimisation approach can be found in [1, 7] and references given therein.

3.1 Optimal Problem Formulation

The optimisation problem is to find the PHEV control variables in each discrete time step in order to minimise the cumulative fuel consumption, while satisfying the state- and control variables-related constraints, as well as a requirement on the value of state variable in the final time step. By introducing the substitutions for the state variable x, control vector **u** and external input vector **v**:

$$x = SoC, \qquad \mathbf{u} = [\tau_e \; h]^T, \qquad \mathbf{v} = [\tau_w \; \omega_w]^T, \tag{7}$$

the following discrete-time cost function including cumulative fuel consumption is set:

$$J = \sum_{k=1}^{N} F(x_k, \mathbf{u}_k, \mathbf{v}_k, k), \tag{8}$$

$$\begin{aligned} F(x_k, \mathbf{u}_k, \mathbf{v}_k, k) = \; & \dot{m}_f \Delta T + K_g\{H^-(x_k - SoC_{min}) + H^-(SoC_{max} - x_k)\} \\ & + K_g\{H^-(P_{batt}^{max} - P_{batt,k}) + H^-(P_{batt,k} - P_{batt}^{min})\} \\ & + K_g\{H^-(\tau_{e,k} - \tau_e^{min}) + H^-(\tau_e^{max} - \tau_{e,k})\} \\ & + K_g\{H^-(\omega_{e,k} - \omega_e^{idle}) + H^-(\omega_e^{max} - \omega_{e,k})\} \\ & + K_g\{H^-(\tau_{MG,k} - \tau_{MG}^{min}) + H^-(\tau_{MG}^{max} - \tau_{MG,k})\} \\ & + K_g\{H^-(\omega_{MG,k} - \omega_{MG}^{idle}) + H^-(\omega_{MG}^{max} - \omega_{MG,k})\}, \end{aligned} \tag{9}$$

where k denotes the discrete time step, N is the total number of discrete time steps, and ΔT is the discretisation time step. Apart from the fuel consumption within discrete time step, $\dot{m}_f \Delta T$, additional terms aimed to penalise violation of different constraints are included into Eq. (9). The function $H^-(.)$ represents the inverted Heaviside function which is equal to 1 when its argument is negative, while otherwise it equals 0. The factor K_g is weighting factor which is set to a relatively large value (here $K_g = 10^{12}$) in order to avoid constraints violation. The state equation given by Eq. (5) can be discretized in time to assume difference equation form:

$$x_{k+1} = f(x_k, \mathbf{u}_k, \mathbf{v}_k, k), \qquad k = 0,1, \dots, N-1 \tag{10}$$

The initial state variable at $k = 0$ and final state variable at $k = N$ are defined as

$$x_0 = SoC_i, \quad x_f = SoC_f. \tag{11}$$

An additional term J_f penalising the deviation of the final SoC from the target value SoC_f is included in the cost function (8), so that the final optimisation problem reads

$$\min_{\mathbf{u}_k} \left(J_f + \sum_{k=1}^{N} F(x_k, \mathbf{u}_k, \mathbf{v}_k, k) \right), \tag{12}$$

$$J_f = K_f\left(SoC_f - x_N\right)^2 = K_f\left(SoC_f - f(x_{N-1}, \mathbf{u}_{N-1}, \mathbf{v}_{N-1})\right)^2, \tag{13}$$

where K_f denotes a weighting factor (here $K_f = 10^6$).

The above-formulated optimisation problem is solved by using a dynamic programming (DP), which provides globally optimal results for given discretisation resolution of the state and control variables (set as a trade-off between computational efficiency and the optimisation accuracy).

3.2 Optimisation Results

DP optimisations of PHEV control variables are conducted for the blended regime and different repeating driving cycles defined in Fig. 4, where DUB1 driving cycle is considered both for zero and varying road grade. The driving cycles are repeated three times to provide discharging the battery to its minimum allowable SoC level which is set here to 30%. The optimised SoC trajectories given in dependence of distance travelled (blue colour plots in Fig. 5) are close to linear profile, which represents the minimum

length between two SoC boundary points. This is confirmed by the values of correlation index K (also given in Fig. 5 and obtained by using Matlab function *corrcoef(.)*), which are close to 1. The linear trend is slightly deteriorated in the case when the road grade is introduced (Fig. 5a), which is also reflected in somewhat reduced correlation index. In this case low frequency oscillations appear in the SoC trajectory, which are caused by the battery recharging during regenerative braking on negative slopes.

The observed, approximately linear optimal pattern of SoC trajectory can serve as a basis for synthesis of SoC reference trajectory applied within a powertrain control strategy for the blended regime and the case when a trip distance is known in advance [1, 6].

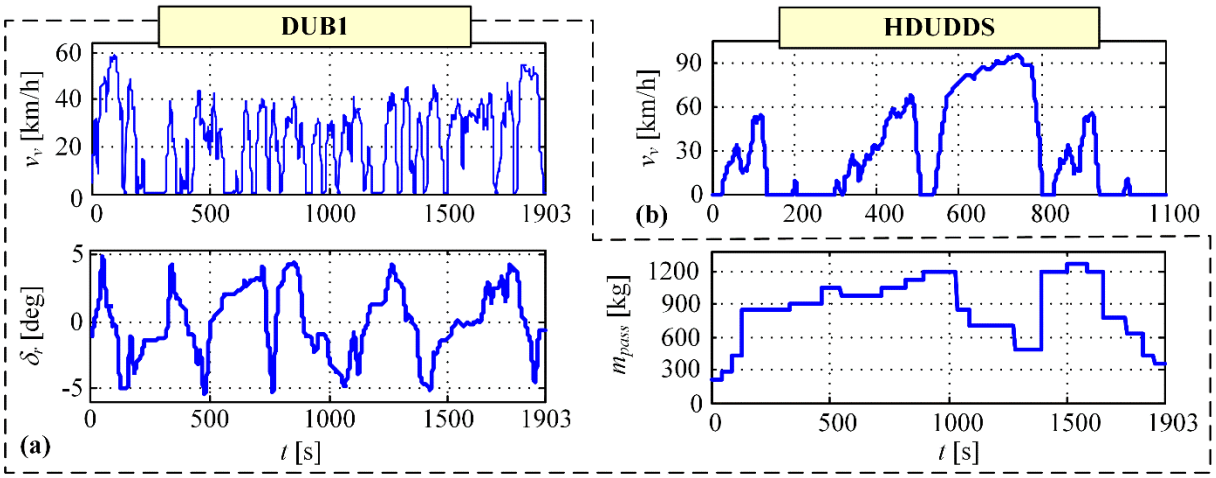

Figure 4: City bus driving cycle including vehicle velocity (v_v), road grade (δ_r) and passenger mass (m_{pass}) time profiles recorded in the city of Dubrovnik (DUB1) (a), and velocity time profile for heavy duty UDDS driving cycle (HDUDDS) which assumes zero road grade and no passengers (b).

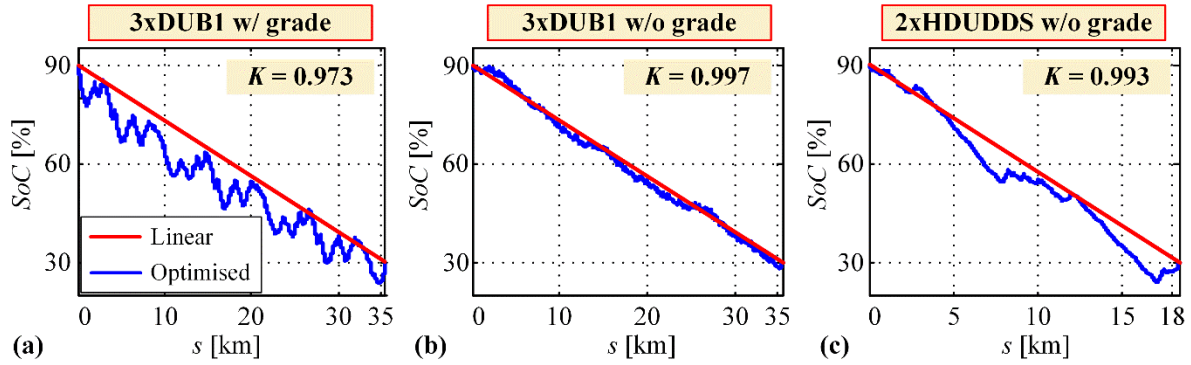

Figure 5: Optimal SoC trajectories obtained by DP algorithm in blended regime and repeating driving cycles from Fig. 4 (DUB1 cycle is considered with varying road grade and zero grade, with the same passenger mass profile in both cases).

3.3 Generation and analysis of SoC trajectories of different length

Based on the results presented in Fig. 5 it can be hypothesised that the optimality is closely related to the SoC trajectory length, i.e. that the shortest-length trajectory is optimal. In order to test this hypothesis, the optimal SoC trajectories of different length are generated by introducing the following additional SoC soft constraint to the cost function included in Eq. (12)

$$J_{SoC,add} = \sum_{j=1}^{N_j} \left(SoC_{constr,j} - x_j\right)^2 = \sum_{j=1}^{N_j} K_{SoC} \left(SoC_{constr,j} - f\left(x_{j-1}, \mathbf{u}_{j-1}, \mathbf{v}_{j-1}\right)\right)^2, \quad (14)$$

which penalises the deviation of SoC from several (N_j) prescribed values $SoC_{constr,j}$ in the j^{th} discrete time steps (the weighting factor K_{SoC} is set to $5 \cdot 10^5$).

Apart from the total fuel consumption V_f, the total electric energy losses $E_{EL,loss}$ consisting of battery losses $E_{batt,loss}$ and M/G machine losses $E_{M/G,loss}$ are also considered in this analysis:

$$E_{EL,loss} = E_{batt,loss} + E_{M/G,loss}\,. \tag{15}$$

The battery losses are dissipated as a heat on its internal resistance R and have quadratic dependence with respect to battery current I_{batt} (i.e. $\int i_{batt}^2 R dt$), while the M/G machine losses depend on the efficiency η_{MG} (see Fig. 2b).

The normalised SoC trajectory length is calculated as

$$L_{SoC,norm} = \sum_{k=1}^{N} \sqrt{\Delta SoC_k^2 + \left(\frac{\Delta s_k}{s_f}\right)^2}\,, \tag{16}$$

where ΔSoC_k and Δs_k represent the difference of SoC and travelled distance between two consecutive time steps (i.e. $\Delta SoC_k = SoC_k - SoC_{k-1}$, $\Delta s_k = s_k - s_{k-1}$), respectively, while s_f denotes the total travelled distance.

Fig. 6a shows SoC trajectories obtained by DP optimisations for different randomly chosen SoC constraints given by Eq. (14) and the case of 3xDUB1 w/o road grade (see Fig. 5b). The same plot also includes some characteristic SoC trajectories, which are explained in what follows. The SoC trajectory denoted as BLND corresponds to the case where no additional SoC constraint is included in the cost function in Eq. (12), and this trajectory corresponds to the one shown in Fig. 5b. In the case of CD/CS trajectory, the battery is first depleted under whenever-possible electric driving (CD) until the predefined low level of SoC is reached, which is then sustained by means of hybrid driving (CS). In the case of CS/CD trajectory the order of CD and CS regimes is reversed. The SoC trajectory of maximum length is denoted by *max* $L_{SoC,norm}$ label. Different metrics for each of the SoC trajectories from Fig. 6a are shown in Figs. 6b-6d.

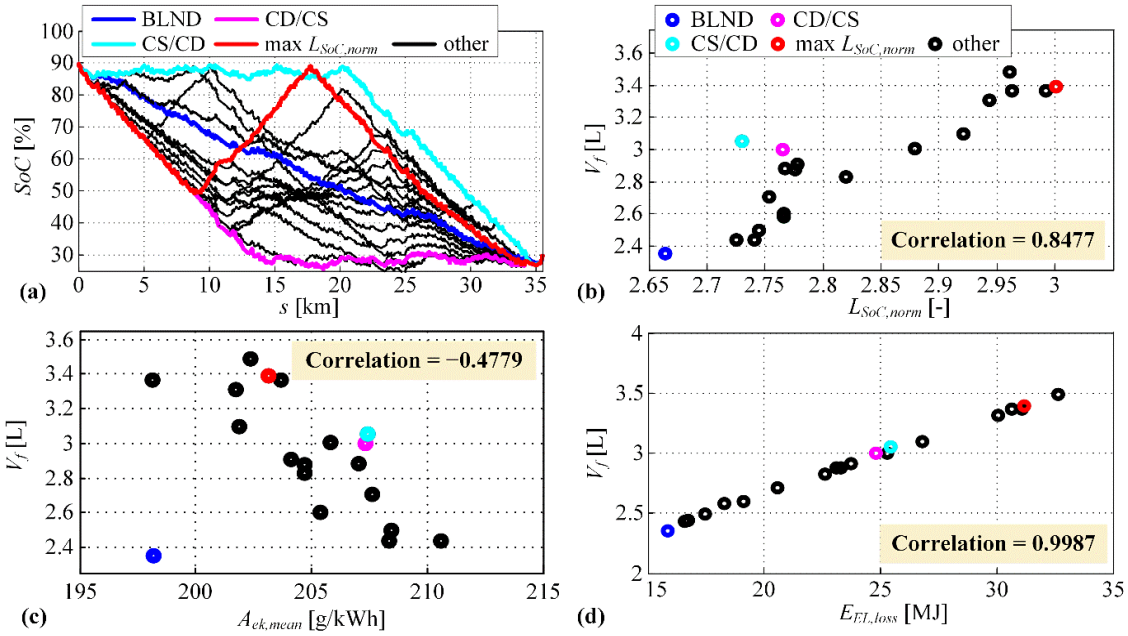

Figure 6: Set of optimal DP-based SoC trajectories of different length obtained by imposing additional SoC constraint (14) (a); and corresponding total fuel consumption V_f shown versus normalised SoC trajectory length $L_{SoC,norm}$ (b), mean engine specific fuel consumption $A_{ek,mean}$ (c), and total electric energy losses $E_{EL,loss}$ (d) (3xDUB1 w/o road grade driving cycle is used).

Fig. 6b reveals that the total fuel consumption V_f highly correlates with the SoC trajectory length $L_{SoC,norm}$ (i.e. larger $L_{SoC,norm}$ corresponds to larger V_f). Since all SoC trajectories end up in the same value (SoC_f = 0.3), the observed variations in the fuel consumption for different SoC trajectories may be caused by: (i) different distribution of operating points in the engine specific fuel consumption map, and (ii) different total electrical losses (15). In order to understand these causes better, the total fuel consumptions V_f are shown versus the mean engine specific fuel consumptions $A_{ek,mean}$ in Fig. 6c, and versus the total electrical losses $E_{EL,loss}$ in Fig. 6d. The results shown in Fig. 6c reveal that the cause (i) may be discarded since the larger total fuel consumption often corresponds to lower mean specific fuel consumption. On the other hand, Fig. 6d confirms that the increased fuel consumption is predominantly caused by the increased total electrical losses (the correlation index is very close to 1). BLND-case SoC trajectory has minimum length and results in minimum fuel consumption, while $maxL_{SoC,norm}$-case SoC trajectory (obtained for N_j = 2 in Eq. (14)) has the maximum length and results in maximum fuel consumption (Fig. 6b).

Based on the presented analysis it can be concluded that the observed optimal pattern related to SoC trajectory length minimization (i.e. linear-like trend) is closely related to minimisation of the electrical losses. More detailed analyses are presented in the following section.

4 Analysis of Optimal SoC Trajectory Patterns

This section is aimed to further explain the observed DP-based optimal SoC trajectory patterns, starting by an analysis of the optimal operation of a battery-only system and following by an analysis of the whole powertrain including the engine, M/G machine and battery.

4.1 Simplified Case of Minimizing Solely Battery Energy Losses

First, the problem of discharging battery from the initial SoC value SoC_i (here SoC_i = 0.9) to some predefined final value SoC_f (here SoC_f = 0.3) with the aim of maximising energy drawn from the battery is considered. The useful energy drawn is maximised if the internal battery energy losses $E_{batt,loss}$ are minimised:

$$\min E_{batt,loss} = \min \int_0^{t_f} P_{batt,loss} dt = min \int_0^{s_f} \frac{P_{batt,loss}}{v_v} ds, \qquad \text{s.t.} \int_0^{t_f} \dot{SoC} dt = SoC_f - SoC_i \tag{17}$$

Similarly, the derivative of SoC with respect to travelled distance is expressed as

$$\frac{dSoC}{ds} = -\frac{I_{batt}(t)}{Q_{max}} \frac{1}{v_v}, \tag{18}$$

The battery power losses equal $P_{batt,loss} = I_{batt}^2 R(SoC)$, which when combining with Eqs. (17) and (18) gives the following optimisation problem expressed through the argument $dSoC/ds$:

$$\min_{I_{batt}} \int_0^{s_f} \frac{I_{batt}^2 R(SoC)}{v_v} ds = \min_{\frac{dSoC}{ds}} \int_0^{s_f} Q_{max}^2 R(SoC) \left(\frac{dSoC}{ds}\right)^2 v_v ds, \ \text{s.t.} \int_0^{t_f} \dot{SoC} dt = SoC_f - SoC_i \tag{19}$$

Discretisation of Eq. (19) results in the problem of determining optimal ΔSoC_r on r^{th} route segment with length Δs_r

$$\min_{\frac{\Delta SoC_r}{\Delta s_r}} \sum_{r=1}^{N_R} R(SoC_r) \left(\frac{\Delta SoC_r}{\Delta s_r}\right)^2 v_{v,r} \Delta s_r, \qquad \text{s.t.} \sum_{r=1}^{N_R} \Delta SoC_r = SoC_f - SoC_i, \tag{20}$$

where Q_{max} is omitted since it is constant and does not have impact on the optimisation problem solution. Next, the following substitution can be introduced

$$y_r{}^2 = R(SoC_r)\left(\frac{\Delta SoC_r}{\Delta s_r}\right)^2 v_{v,r}\Delta s_r, \tag{21}$$

leading to

$$\min_{y_r} \sum_{r=1}^{N_R} y_r{}^2 . \tag{22}$$

Since the quadratic function $(.)^2$ is convex, the following expression based on Jensen's inequality can be established

$$\frac{\sum_{r=1}^{N_R} y_r{}^2}{N_R} \geq \left(\frac{\sum_{r=1}^{N_R} y_r}{N_R}\right)^2, \tag{23}$$

where the numerator on the left-hand side of Eq. (23) corresponds to the cost function of the optimisation problem (22). Now, the minimum of the left-hand side of Eq. (23) (corresponding to equality of the left-hand side and right-hand side terms) is achieved for the constant value of y_r for all route segments. By combining the equality constraint from Eq. (20) (i.e. $\sum_{r=1}^{N_R} \Delta SoC_r = SoC_f - SoC_i$) related to the SoC boundary values and posing y_r to be constant, the following expression for the optimal SoC depletion on r^{th} route segment can be obtained

$$\frac{\Delta SoC_r}{\Delta s_r} = \frac{SoC_f - SoC_i}{\sqrt{R(SoC)v_{v,r}\Delta s_r}\sum_{j=1}^{N_R}\frac{\Delta s_j}{\sqrt{R(SoC_j)v_{v,j}\Delta s_j}}}. \tag{24}$$

By assuming constant vehicle velocity v_v, constant internal resistance R, and constant length of each route segment Δs, the expression (24) leads to $\Delta SoC_r/\Delta s_r = (SoC_f - SoC_i)/s_f$, where s_f represents the total travelled distance. In that case the optimal operation would be to discharge the battery with constant SoC depletion rate, i.e. the SoC trajectory would follow the linear trend and have the minimum length.

The same battery discharging problem is further analysed numerically by using DP algorithm to study the impact of varying battery parameters on SoC trajectory shape. Fig. 7 shows SoC trajectories obtained by constant SoC depletion rate (SoC_{lin}) and by DP optimisations for: (i) the constant battery parameters (the mean values from Fig. 3b are used), and (ii) the SoC-dependent battery parameters (Fig. 3b). In the case of

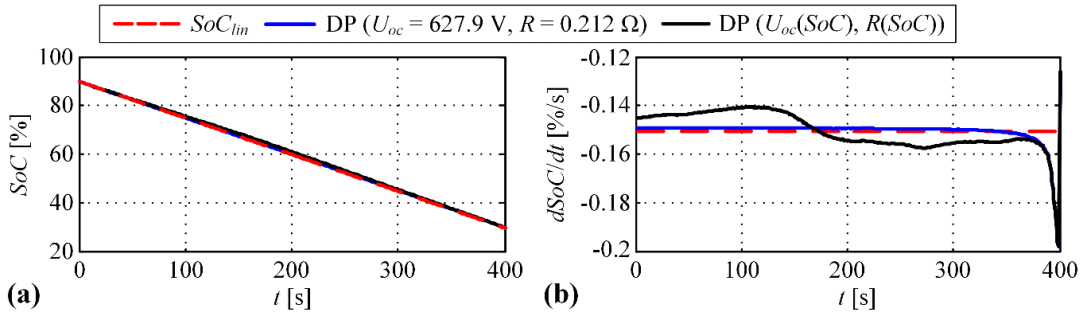

Figure 7: SoC trajectories obtained by constant discharging rate (SoC_{lin}) and DP optimisation (a) and corresponding discharging rates (b), where DP results correspond to cases of constant and SoC-dependent battery parameters.

constant battery parameters, the optimal operation is related to a constant SoC depletion rate (Fig. 7b; slight deviation from the constant value in the case of DP occurs due to discretisation effects and the requirement on the final SoC value). It can be observed from Fig. 7a that the impact of variable battery parameters on the optimal SoC trajectory shape is negligible. The slight deviation from the constant SoC depletion rate in the case of variable battery parameters (Fig. 7b) is caused by the SoC dependence of internal battery resistance R; namely, slightly lower absolute values of $dSoC/dt$ are observed until SoC falls around 75%, because the resistance R has somewhat larger values for SoC > 75% than in the range from 30% to 65% (see Fig. 3b).

4.2 More Realistic Case of Minimizing Fuel Consumption

The analysis is extended here to the overall powertrain, which includes the engine, M/G machine, transmission, and battery (see Fig. 1a). In order to study the optimal SoC trajectory with respect to fuel consumption minimization while discharging the battery (i.e. from 90% to 30%), the fuel consumption rate $\dot{m}_f$ is expressed in dependence on SoC depletion rate $\dot{SoC}$ for different values of the battery SoC, power demand P_d, and the engine speed ω_e:

$$\dot{m}_f = g\left(\frac{dSoC}{dt}, SoC, P_d, \omega_e\right). \tag{25}$$

The optimal solution for $\dot{SoC}$ which minimises the fuel consumption can be found analytically if the function g in Eq. (25) is convex, under assumption of constant values of P_d, SoC, and ω_e (i.e. constant vehicle velocity). It can be shown that the optimality is achieved if $\dot{SoC}$ is kept constant during whole driving cycle and set to the value which would discharge the battery to the predefined minimum value (the same reasoning as in the case of deriving optimal SoC depletion in Eq. (24)). The analysis is given here in the time domain, and it is equivalent to the travelled distance domain considered in previous sections because of the constant vehicle velocity assumption considered here.

Fig. 8a shows the graphical representation of the function (25) for several P_d values and for SoC = 50%. The corresponding second derivatives are positive over the whole range thus confirming the convexity of the analysed functions (Fig. 8b). This convexity analysis is also conducted for a wide set of P_d and ω_e values, and the results are shown in Fig. 9 (the function is categorised as non-convex if its second derivative is not strictly positive). According to the results from Fig. 9, the function g in Eq. (25) is convex for a majority of P_d and ω_e values.

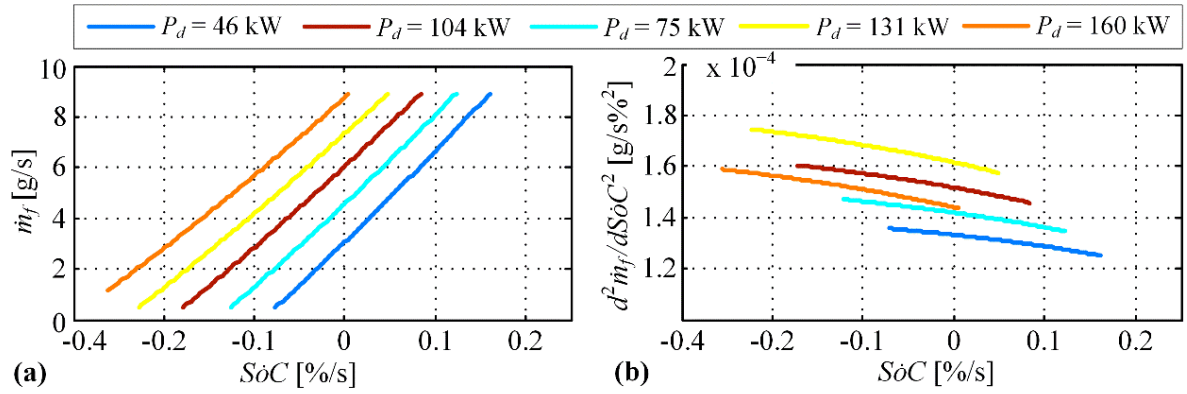

Figure 8: Fuel consumption rate $\dot{m}_f$ vs. SoC depletion rate $\dot{SoC}_f$ (a), and 2nd derivative of $\dot{m}_f$ vs. $\dot{SoC}_f$ curve (b), given for several values of demanded power (P_d), and engine speed ω_e = 184 rad/s and SoC = 50%.

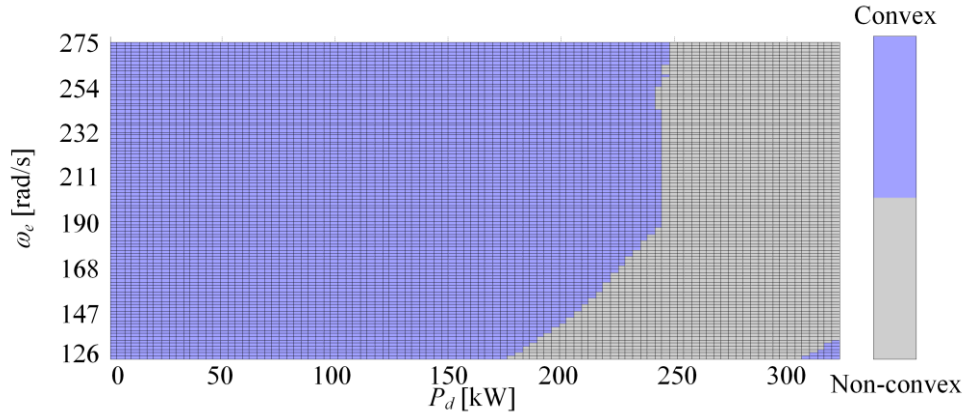

Figure 9: Character of $\dot{m}_f$ vs. $\dot{SoC}$ dependence (convex or non-convex) for a wide range of engine speeds ω_e and driver power demands P_d for the case of SoC = 0.5.

These effects are further illustrated and analysed for the particular ω_e and P_d values for two engine fuel consumption characteristics (g/s): (i) the original one (obtained from Fig. 2a by using Eq. (4)) resulting in the function (25) to be convex, and (ii) the modified one resulting in the function (25) to be concave (see Fig. 10).

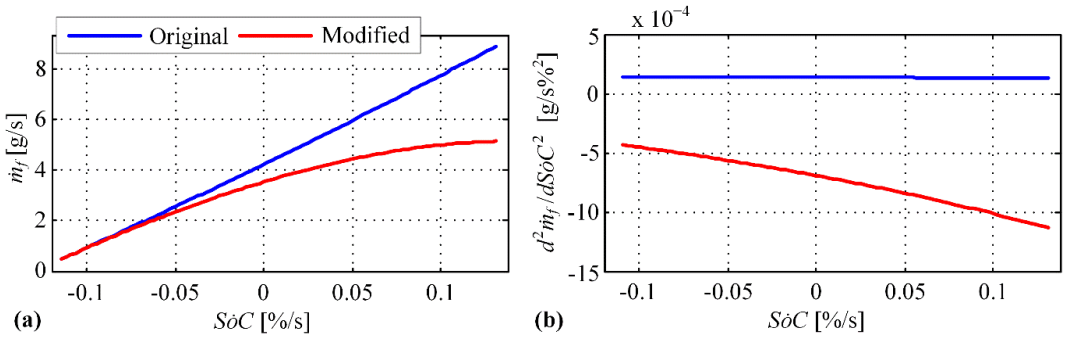

Figure 10: Illustration of original (convex) and modified (concave) engine fuel consumption rate $\dot{m}_f$ with respect to SoC depletion rate $\dot{SoC}$ (a), and the corresponding 2nd derivatives (b) for the case of SoC = 50%, v_v = 86 km/h, ω_e = ω_{MG} = 184 rad/s, P_d = 79.7 kW.

Three different scenarios of battery discharging to the predefined low value are considered (see the related operating points and profiles in Fig. 11):

(i) **OP1** – power demand P_d is partly satisfied by the engine and partly by the electric machine M/G (operating points are kept constant during the whole operation; constant $\dot{SoC} < 0$),

(ii) **OP2** – **Phase 1**: power demand P_d is completely satisfied by the engine ($\dot{SoC} = 0$), **Phase 2**: power demand P_d is completely satisfied by the electric machine M/G (constant $\dot{SoC} < 0$)

(iii) **OP3** – **Phase 1**: power demand P_d is completely satisfied by the engine which also provides additional power to recharge the battery (constant $\dot{SoC} > 0$), **Phase 2**: power demand P_d is completely satisfied by the electric machine M/G (constant $\dot{SoC} < 0$).

From the standpoint of lower engine specific fuel consumption and regardless of type of engine fuel consumption characteristic (original or modified), Scenario OP2 is preferable over Scenario OP1, and Scenario OP3 is preferable over Scenario OP2 (see Figs. 11a and 11b). However, from the standpoint of overall powertrain fuel consumption, Scenario OP1 related to linear SoC trajectory should be optimal if the function $\dot{m}_f$ vs. $\dot{SoC}$ is convex (as it is the case with the original characteristic in Fig. 10a), while it should be suboptimal in the case of non-convex function (modified characteristic in Fig. 10a). This is confirmed by the results presented in Fig. 12, where the comparative fuel consumption time profiles are shown for different scenarios. This finding can be explained by the fact that it is advantageous to place the engine operating point to somewhat larger specific engine fuel consumption (OP1 vs. OP2 and OP3) in the case of

original engine characteristic (see Fig. 11a), and thus avoid relatively large total electrical losses whose increase is progressive with the M/G and battery power (Fig. 11c). In this case the optimal SoC trajectory is that of minimum length. However, in the case of modified engine characteristic, where the difference in the specific fuel consumption between OP2 vs. OP1 and OP3 vs. OP2 is more significant than in the original case (Fig. 11a), it is advantageous to move the engine operating point in reduced specific fuel consumption region (OP3 and OP2; see Fig. 11a and also Fig. 11b) despite the increased electrical losses in Phase 2 (Fig. 11c).

The above analysis contributes to understanding of the tendency of optimal SoC trajectories to be of minimum length (as observed in Fig. 5), taking into account that the function g in Eq. (25) is originally convex in a great majority of (typical) operating region (Fig. 9). Certain deviations of the SoC trajectories in Fig. 5 from the minimum length may be explained by the fact that the assumption on operating parameters (i.e. constant P_d, SoC, and ω_e) is not satisfied for realistic driving cycles.

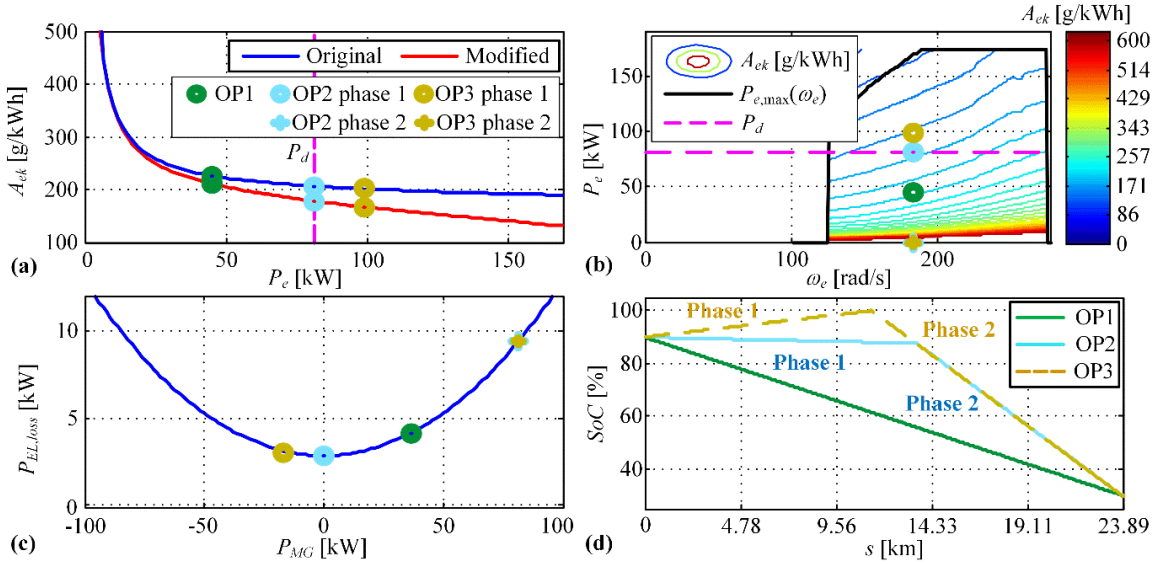

Figure 11: Illustration of three different operating scenarios (the same operating conditions as in Fig. 10: SoC = 50%, v_v = 86 km/h, $\omega_e = \omega_{MG}$ = 184 rad/s, P_d = 79.7 kW).

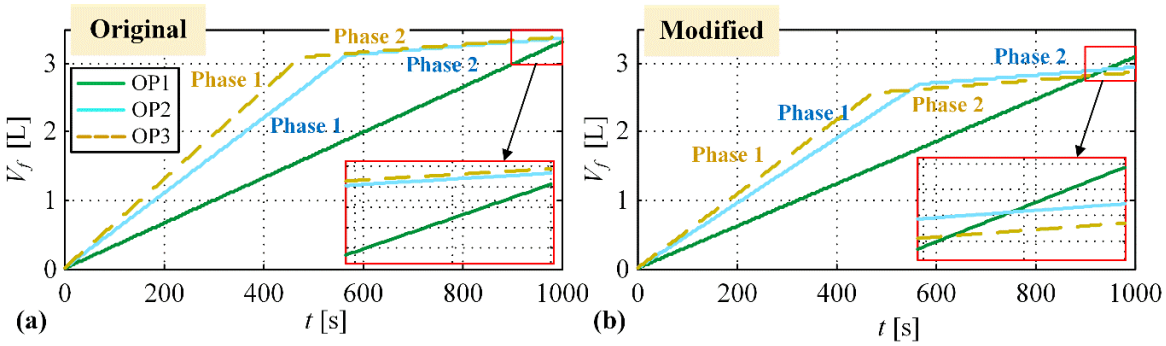

Figure 12: Comparative cumulative fuel consumption time profiles for different operating scenarios for original (a) and modified engine fuel consumption characteristic (b).

5 Conclusion

The paper has dealt with analysis of the optimal battery state-of-charge (SoC) trajectory for the blended operating regime of a parallel plug-in hybrid electric vehicle (PHEV). The analysis is based on optimal control results obtained by using dynamic programming optimisations for various driving cycles and based on a backward-looking powertrain model. It has been found that the optimal SoC trajectories (when expressed with respect to distance travelled) tend to have nearly-linear shape for different driving cycles, which corresponds to the minimum SoC trajectory length. The minimum SoC trajectory length has been

proven to be optimal both analytically and numerically for a simplified battery-only system based on battery power loss minimisation. The analysis has been extended to the whole powertrain including the engine, electric machine and battery, where the main aim was to minimise the total fuel consumption. It has been shown that the linear SoC trajectory is also optimal for the whole powertrain in the actual case of convex shape of fuel mass flow vs. SoC depletion rate characteristic.

The linear SoC trajectory is optimal because of its feature to minimise the total electrical losses and because of flexibility in setting the engine operating points due to a relatively flat engine specific fuel consumption vs. engine power characteristic in a wide range. It has also been demonstrated that when modifying the engine specific fuel consumption characteristic to some extent, the optimal SoC trajectory can have significantly different pattern than the minimum-length linear one.

Acknowledgments

It is gratefully acknowledged that this work has been supported by Croatian Science Foundation under the project No. IP-2018-01-8323 (Project Acronym: ACHIEVE), while the initial research effort on the topic had been done through Interreg CE project SOLEZ.

References

[1] B. Škugor, M. Cipek, J. Deur, *Control Variables Optimization and Feedback Control Strategy Design for the Blended Operating Mode of an Extended Range Electric Vehicle*, SAE International Journal of Alternative Powertrains, SAE paper # 2014-01-1898, Vol. 3, No. 1, pp. 152-162., 2014.

[2] H. Yu, M. Kuang, R. McGee, *Trip-Oriented Energy Management Control Strategy for Plug-In Hybrid Electric Vehicles*, IEEE Transactions on Control Systems Technology, Vol. 22 (4), pp. 1323–1336, 2014.

[3] S. Onori, L. Tribioli, *Adaptive Pontryagin's Minimum Principle supervisory controller design for the plug-in hybrid GM Chevrolet Volt*, Applied Energy, Vol. 147, pp. 224-234, 2015.

[4] J. Soldo, B. Škugor, J. Deur, *Optimal Energy Management Control of a Parallel Plug-in Hybrid Electric Vehicle in the Presence of Low Emission Zones*, WCX SAE World Congress Experience, Detroit, Michigan, 2019.

[5] J. Soldo, B. Škugor, J. Deur, *Optimal Energy Management and Shift Scheduling Control of a Parallel Plug-in Hybrid Electric Vehicle*, Powertrain Modelling and Control Conference (PMC 2018), Loughborough, UK, 2018.

[6] B. Škugor, M. Cipek, D. Pavković, J. Deur, *Design of a power-split hybrid electric vehicle control system utilizing a rule-based controller and an equivalent consumption minimization strategy*, Proceedings of the Institution of Mechanical Engineers, Part D, Journal of Automobile Engineering, Vol. 228, No. 6, pp. 631-648, 2014.

[7] M. Cipek, B. Škugor, M. Čorić, J. Kasać, J. Deur, *Control variable optimisation for an extended range electric vehicle*, International Journal of Powertrains, Vol. 5 (1). pp. 30-54, 2016.

Authors

Branimir Škugor is a postdoctoral researcher at the University of Zagreb. He received his Ph.D. degree in Mechanical Engineering from the same university in 2016. He has participated in several projects supported by Croatian Science Foundation, European Commission, and Ford Motor Company. His research interests include advanced control of hybrid electric vehicle powertrains, modelling and charging optimization of electric vehicle fleets, synthesis of driving cycles, and machine learning with automotive applications.

Jure Soldo is a PhD student at the University of Zagreb-FMENA working on the European INTEREG project entitled “Smart Solutions supporting Low Emission Zones and other low-carbon mobility policies in EU cities”. His research interests relate to modelling and control of plug-in hybrid electric vehicles.

Joško Deur is a Full Professor at the University of Zagreb, where he teaches courses in electrical machines and servodrives, digital control systems, and automotive mechatronics. In 2000, he spent a year with Ford Research Laboratory, Dearborn, MI, as a postdoctoral scholar. Professor Deur has led numerous projects including those supported by Ford Motor Company and Jaguar Cars Ltd. His main research interests include modelling and control of automotive systems and control of electrical servodrives.